Precise percolation thresholds of two-dimensional random systems comprising overlapping ellipses

Jiantong Li* and Mikael Östling

KTH Royal Institute of Technology, School of Information and Communication Technology, *Electrum 229, SE-164 40 Kista, Sweden*

*Email: jiantong@kth.se

This work explores the percolation thresholds of continuum systems consisting of randomly-oriented overlapping ellipses. High-precision percolation thresholds for various homogeneous ellipse systems with different aspect ratios are obtained from extensive Monte Carlo simulations based on the incorporation of Vieillard-Baron's contact function of two identical ellipses with our efficient algorithm for continuum percolation. In addition, we generalize Vieillard-Baron's contact function from identical ellipses to unequal ellipses, and hence extend the Monte Carlo algorithm to heterogeneous ellipse systems where the ellipses have different dimensions and/or aspect ratios. Based on the concept of modified excluded area, a general law is verified for precise prediction of percolation threshold for many heterogeneous ellipse systems. In particular, the study of heterogeneous ellipse systems gains insight into the apparent percolation threshold symmetry observed earlier in systems comprising unequal circles [Physica A 343, 343 (2004)].

I. INTRODUCTION

For a long time, systems consisting of overlapping or hard ellipses have received a great deal of attention in theoretical studies [1–6]. Recently, the extensive research on percolation systems based on low-dimensional nanoparticles, such as two-dimensional (2D) layered materials (graphene, MoS_2, etc. [7–10]) and one-dimensional fiber-like nanostructure (carbon nanotubes, metal nanowires, etc. [11–13]), extends the interest in overlapping ellipse systems to many practical applications. Like ellipsoids in three-dimensional (3D) systems [14], ellipses represent the general object shape in 2D systems, ranging from extremely anisotropic fibers or rods to isotropic disks. Up to date, however, there are still some fundamental issues concerning ellipse percolation not well addressed. One the one hand, the reported percolation thresholds of homogeneous ellipse systems are still at low precision[1], not matching their counterparts, such as the systems comprising sticks [15,16], disks (circles) [17], and rectangles [18]. On the other hand, most simulation [1] and analytic [2] work employs the contact function proposed by Vieillard-Baron [5] (hereafter referred to as VB contact function) to efficiently determine the overlapping status of two identical ellipses. However, the present form of VB contact function only applies to identical ellipses, restricting relevant studies to homogeneous ellipse systems.

This work aims to advance the field and is outlined as follows. Section II explores the high-precision percolation thresholds for homogeneous systems with various ellipse aspect ratios. Section III generalizes VB contact function from identical ellipses to unequal ellipses and investigates heterogeneous systems. Relevant topics are also discussed, including excluded area [18] and apparent symmetry of percolation threshold in systems of unequal object shapes [19]. Section IV summarizes all the conclusions.

II. HOMOGENEOUS ELLIPSE SYSTEMS

In order to obtain high-precision percolation thresholds for homogeneous ellipse systems, we conduct extensive Monte Carlo simulations (each reported percolation threshold requires

5000 - 40000 core-hours of computation) through an efficient algorithm which integrates the VB contact function [5] into our prior continuum percolation algorithm [15,18] . The algorithm, based on the combination between the fast Newman-Ziff algorithm [20] and the subcell concept [21], is identical to that for stick and rectangle percolation [15,18] except that the bonding criterion is determined by the VB contact function. Briefly, we begin with a blank system (square area) and continuously add ellipses into the system until a cluster, which comprises connecting ellipses, percolates the system. An ellipse of known (fixed) major semi-axis a, minor semi-axis b and hence aspect ratio $r = a/b$, is simply stored as the combination of a random point (x, y) as its center with a random angle θ as its orientation, and can be denoted as E: [(a, b): (x, y), θ]. As shown in Fig. 1, The system of size L is divided into $L \times L$ subcells (squares), each of which has length $l = 2a$ (for simplicity, we set $l \equiv 1$ and hence $a = 1/2$). During the simulations, each ellipse is registered into a subcell where its center locates so that it is only necessary to check its connectivity with those ellipses locating in the same and eight neighboring subcells. The connectivity between any two identical ellipses, E_1: [(a, b): (x_1, y_1), θ_1] and E_2: [(a, b): (x_2, y_2), θ_2], can be determined by the VB contact function [5],

$$\Psi = 4\left(f_1^2 - 3f_2\right)\left(f_2^2 - 3f_1\right) - \left(9 - f_1 f_2\right)^2, \tag{1a}$$

where ($\alpha = 1, 2$)

$$f_\alpha = 3 + \left(a/b - b/a\right)^2 \sin^2\Delta\theta - a^{-2}\left(\Delta x\cos\theta_\alpha + \Delta y\sin\theta_\alpha\right)^2 - b^{-2}\left(\Delta y\cos\theta_\alpha - \Delta x\sin\theta_\alpha\right)^2, \tag{1b}$$

with $\Delta x = x_2 - x_1$, $\Delta y = y_2 - y_1$, and $\Delta\theta = \theta_2 - \theta_1$. The two ellipses intersect (overlap) if and only if $\Psi < 0$ or all Ψ, f_1, and f_2 are positive (i.e., $\Psi > 0$, $f_1 > 0$, and $f_2 > 0$).

For free boundary conditions (FBC), the system percolates (spans) when a cluster connects both the two opposite boundaries, e.g., the two vertical boundary lines, $x = 0$ and $x = L$, in Fig. 1. To facilitate checking the presence of a spanning cluster, before adding the ellipses,

we introduce into the blank system two separate "fake" ellipses, named as LEFT and RIGHT, which actually represent the two boundary lines $x = 0$ and $x = L$, respectively. During the cluster evolution, the two ellipses play the same role as a normal ellipse except that they intersect with other ellipses under a different bonding criterion: When a new ellipse E_0: [(a, b), (x_0, y_0), θ_0] locates in the left (right) boundary subcells (shaded subcells in Fig. 1), before checking its connectivity with other ellipses, we test its intersection with the LEFT (RIGHT) ellipse, i.e., the boundary line $x = 0$ ($x = L$), through the criterion

$$\left(x - x_0\right)^2 \le b^2 \sin^2\theta_0 + a^2 \cos^2\theta_0 . \qquad (2)$$

If Eq. (2) is satisfied, E_0 intersects the LEFT (or RIGHT) ellipse and is attached to the cluster of the latter. Once the LEFT and RIGHT ellipses lie in the same cluster, the system percolates.

The rest of the simulation procedure is identical to that for rectangle systems [18], such as the pre-screening of two ellipses through checking their center distance before being examined by the VB contact function, and convolution of the simulated spanning probability with Poisson distribution. After a number of simulation runs, the spanning probability $R(N, L)$ is obtained for systems of size L at any arbitrary ellipse number density N. The percolation threshold N_c can be extracted from the convergence [22,23]

$$N_{0.5}(L) - N_c \propto L^{-1-1/\nu}, \qquad (3)$$

where $N_{0.5}(L)$ is defined through $R[N_{0.5}(L), L] = 0.5$ and $\nu = 4/3$ is the critical correlation-length exponent. According to our simulation results, $N_{0.5}(L)$ for all systems (L = 48, 64, 72, 88, 128 and 256, each data is based on > 10^7 simulation runs) of the same ellipse ratio r converges to N_c in excellent agreement with Eq. (3). Some examples are shown in Fig. 2. The extracted N_c for all the systems studied in this work is listed in Table I where the uncertainty, half-width of the 95% confidence interval, is less than 1×10^{-4}, comparable to those for rectangle systems [18].

Previous studies [16,20] suggest that if a system, of square boundaries and periodic boundary conditions (PBC), has wrapping probability $W[N, L]$, the percolation threshold can be extracted from

$$N_\eta(L) - N_c = L^{-2-1/\nu}, \tag{4}$$

where $N_\eta(L)$ is defined as $W[N_\eta(L), L] = W[N_c, \infty] \equiv W_\infty$. While there are different types of wrapping probabilities [16,20], in this work we only consider the horizontal wrapping probability $W^{(h)}$ which is the probability of wrapping horizontally around the system and $W_\infty^{(h)}$ = 0.521 058 289 248 821 787 848 ... [16,20]. One can see that $N_\eta(L)$ in PBC systems [Eq. (4)] converges to N_c much faster than $N_{0.5}(L)$ in FBC systems [Eq. (3)]. In addition, for PBC ellipse systems, the determination of wrapping probability does not involve the "fake" ellipses and hence the extra bonding criterion of Eq. (2) is not needed. However, in order to reach good statistics for $N_\eta(L)$, much larger number of simulation runs are indispensable [16,20]. Figure 2 also shows the convergence of $N_\eta(L)$ for L = 32, 40, 48, 56, 64, 72, 88, 100 and 128, where each data point is obtained from > 2×10^7 simulation runs. Despite the comparable number of simulation runs, the convergence of $N_\eta(L)$ in PBC systems is much poorer than that of $N_{0.5}(L)$ in FBC systems. Nevertheless, because all $N_\eta(L)$ are very close to N_c even for the smallest system size L = 32 [Figs. 2(c) and 2(d)], the extracted N_c from the PBC systems [Eq. (4)] is comparable or sometimes even superior to those from the FBC systems [Eq. (3)], as shown in Table I. Actually, because of the nearly negligible finite-size effects in PBC systems, it is acceptable to approximate N_c by a single $N_\eta(L)$ with a small L (for example L = 32) when high-precision N_c is not required. This provides an effective way for our studies on heterogeneous ellipse systems in Sec. III. In Table I, we also compare our percolation thresholds with the values reported in previous work. The earlier researches on ellipse systems [1,2,6] did

not employ the Newman-Ziff algorithm or the subcell algorithm, so it was challenging to study large-size systems to effectively address finite-size effects. As a result, only low-precision percolation thresholds can be obtained, as listed in Table I.

In 2D continuum systems, percolation threshold N_c is often assumed to be inversely proportional to the average excluded area A [24], or the product N_cA for all systems varies within a range as narrow as $3.2 \le N_cA \le 4.5$ [25]. In general, the average excluded area between any two randomly-oriented convex plates i and j is [26,27]

$$A_{ij} = S_i + S_j + C_iC_j/2\pi , \tag{5}$$

where S_i and C_i are the area and perimeter of the plate i, respectively. For two identical ellipses with semi-axes a and b ($r = a/b$), Eq. (5) turns to be

$$A_{ii} \equiv A_r = 2\pi ab + C^2/2\pi = 4S_ik_i , \tag{6}$$

where $S_i = \pi ab$ is the ellipse area,

$$k_i = 1/2 + C^2/8\pi ab , \tag{7}$$

and the ellipse perimeter C is [28]

$$C = \pi(a+b)\left(1+\sum_{n=1}^{\infty}\left[\frac{(2n-2)!h^n}{n!(n-1)!2^{2n-1}}\right]^2\right), \tag{8}$$

with $h = (a-b)/(a+b) = (r-1)/(r+1)$. For homogeneous ellipse systems, we set all a = 1/2. Then A_{ii} in Eq. (6) only depends on r, and can be denoted as $A_{ii} \equiv A_r$. In the limit case $r \to \infty$, $b = 0$, $C = 4a = 2$, and hence $A_\infty = 2\pi^{-1}$. Note that A_∞ for ellipse systems is identical to that for rectangle systems [18]. This can be expected since in the limit case $r \to \infty$, both ellipse systems and rectangle systems turn to be stick systems [15].

The products N_cA_r for the ellipse systems are also listed in Table I. It is clear that all of them lies within the predicted region $3.2 \le N_cA_r \le 4.5$ [25], except for the case of $r = 1$ where $N_cA_r = 4.513$, slightly beyond the upper limit. Figure 3 plots the percolation threshold N_c against

the normalized reciprocal excluded area $s \equiv A_r^{-1} / A_\infty^{-1} = 2\pi^{-1} A_r^{-1}$. One can see that N_c monotonically, but not linearly, increases with s. For comparison, N_c for rectangle systems is also plotted in Fig. 3 (note that the wrong formulae for excluded area of rectangles in [18] have been corrected [29,30]). The two kinds of systems have very similar N_c - s relationship, although the small difference is beyond the statistical error in Fig. 3. In order to facilitate future research on the ellipse systems, similar to rectangle systems [18,29], we use a high-order polynomial to fit their N_c - s relation as

$$N_c = f(s) = \sum_{i=1}^{n} c_i s^i \,, \tag{9}$$

where $s = 2\pi^{-1} A_r^{-1}$ and c_i are constant coefficients. When n = 8, perfect fitting (adjusted $R^2 > 1 - 2\times10^{-10}$) can be obtained from nonlinear regression of Eq. (9) to N_c obtained from PBC systems in Table I. The fitted coefficients c_i are listed in Table II. With these c_i, one may predict N_c for ellipse systems of *any r ranging from 1 to* ∞ with maximum uncertainty < 5×10^{-5}, a comparable level to the uncertainty of simulation results in this work. Here n = 8 is the minimum order number to ensure such small uncertainty.

III. HETEROGENEOUS ELLIPSE SYSTEMS

A. Generalized VB contact function

Following the outline in Appendix A of Ref. [5], we derive the generalized contact function for two unequal ellipses E1: [(a_1, b_1): (x_1, y_1), θ_1] and E2: [(a_2, b_2): (x_2, y_2), θ_2], as

$$\Psi = 4\left(f_1^2 - 3f_0 f_2\right)\left(f_2^2 - 3f_1\right) - \left(9f_0 - f_1 f_2\right)^2 , \tag{10a}$$

where

$$f_0 = a_1^2 b_1^2 a_2^{-2} b_2^{-2} \,, \tag{10b}$$

$$f_1 = f_0\Big[1+\left(b_2^2a_1^{-2}+a_2^2b_1^{-2}\right)\sin^2\Delta\theta+\left(a_2^2a_1^{-2}+b_2^2b_1^{-2}\right)\cos^2\Delta\theta \\ -a_1^{-2}\left(\Delta x\cos\theta_1+\Delta y\sin\theta_1\right)^2-b_1^{-2}\left(\Delta y\cos\theta_1-\Delta x\sin\theta_1\right)^2\Big], \quad (10c)$$

and

$$f_2 = 1+\left(a_1^2b_2^{-2}+b_1^2a_2^{-2}\right)\sin^2\Delta\theta+\left(a_1^2a_2^{-2}+b_1^2b_2^{-2}\right)\cos^2\Delta\theta \\ -a_2^{-2}\left(\Delta x\cos\theta_2+\Delta y\sin\theta_2\right)^2-b_2^{-2}\left(\Delta y\cos\theta_2-\Delta x\sin\theta_2\right)^2, \quad (10d)$$

still with $\Delta x = x_2 - x_1$, $\Delta y = y_2 - y_1$, and $\Delta\theta = \theta_2 - \theta_1$. Again, E_1 and E_2 intersect (overlap) if and only if $\Psi < 0$ or all Ψ, f_1, and f_2 are positive.

B. Threshold prediction of binary systems

Integration of the generalized contact function into our Monte Carlo algorithm allows the studies on heterogeneous systems consisting of ellipses with different dimensions and/or aspect ratios. For simplicity, in this work we only investigate binary PBC systems which comprise two different types of ellipses (as illustrated in Fig. 4), and all of their percolation threshold N_c is approximated by $N_\eta(L=32)$. Similar to rectangle systems [18], we denote a binary ellipse system as [(a_1,b_1), x_1; (a_2,b_2), x_2] where x_i (i = 1, 2) is the number fraction of the ith type of ellipses with semi-axes a_i and b_i, respectively, and $x_1 + x_2 = 1$. A group of ellipse systems comprising identical ellipse types (a_1, b_1) and (a_2, b_2) but different number fractions x_i is denoted as {(a_1, b_1); (a_2, b_2)}. The effective average excluded area of [(a_1,b_1), x_1; (a_2,b_2), x_2] is $A_e = x_1^2A_{11} + 2x_1x_2A_{12} + x_2^2A_{22}$ with A_{ij} given by Eq. (6).

Figure 5 plots N_c against $s = 2\pi^{-1}A_e^{-1}$ for a variety of heterogeneous ellipse systems. The $N_c - s$ dependence for most heterogeneous systems agrees well with that [Eq. (9)] for homogeneous systems. However, the deviation is also evident for some heterogeneous systems whose a_1 and a_2 differ significantly from each other, such as the systems {(0.5, 0.05); (0.25, 0.25)}, {(0.5, 0.01); (0.25, 0.25)} and {(0.5, 0.05); (0.3, 0.3)}. For heterogeneous rectangle

systems, we proposed [18] a general law to describe $N_c - s$ relations precisely. Below, we verify that the law also applies to heterogeneous ellipse systems.

In principle, the law is based on the correlation between the two percolation estimates, N_{c1} and N_{c2}, obtained from linearly approximating N_c at the effective average excluded area A_e through the $N_c - s$ relation (for homogeneous systems) at the excluded areas of the two types of ellipses, A_{r_1} and A_{r_2}. In order to obtain accurate estimates, the $N_c - s$ relation should exhibit excellent linearity [29], which, however, is not the case for ellipse systems (as well as rectangle systems), as shown in Fig. 3. We thereby propose the modified excluded area, $\tilde{A}_{ij}$, defined as,

$$\tilde{A}_{ij} = \delta(S_i + S_j) = A_{ij} + \delta\pi(a_i^2 r_i^{-1} + a_j^2 r_j^{-1}), \qquad (11)$$

where δ is a constant. Accordingly, for two identical ellipses (a = 1/2, b = a/r), one has $\tilde{A}_{ij} = (\pi + \delta)/2r + C^2/2\pi$ and $\tilde{A}_{ij} = \pi/2$ (note still $\tilde{A}_{ij} = \pi/2$). It is found that with $\delta = -0.20$, the $N_c - \tilde{A}_{ij}$ relation for homogeneous ellipse systems exhibits significantly better linearity, as also shown in Fig. 3. We rewrite Eq. (9) as

$$N_c = \tilde{b}_0 + \sum_{i=1}^{n} \tilde{b}_i \tilde{x}_i \tilde{x}_i, \qquad (12)$$

where $\tilde{b}_i$ are coefficients, also listed in Table II. Still, with n = 8, Eq. (12) can be used to predict N_c for homogeneous ellipse systems of any aspect ratio ranging from 1 to ∞ at the maximum uncertainty around 1×10^{-4}.

Then, for a binary system [(a_1,b_1), x_1; (a_2,b_2), x_2] with ellipse aspect ratios $r_i = a_i/b_i$, the two percolation threshold estimates, N_{c1} and N_{c2}, can be obtained from the linear approximation as

$$N_{ci} = (2a_i)^{-2}\left[\tilde{b}_0 + \sum_{i=1}^{n} \tilde{b}_i \tilde{x}_i \tilde{x}_i\right], \qquad (13)$$

where $\tilde{\ }$ $\tilde{\ }$ $\tilde{\ }$ $\tilde{\ }$ with $\tilde{\ }$ given by Eq. (10), and $\tilde{\ }$ $\tilde{\ }$ is the first-order derivative of $\tilde{\ }$ $\tilde{\ }$ given by Eq. (11). If the ellipses (a_i, b_i) are sorted so that either $a_1 > a_2$ or $a_1 = a_2$ and $b_1 > b_2$, the percolation threshold of the binary systems is given by

$$N_c = N_{c1}\left(1 - x_2^{\alpha}\right) + N_{c2}x_2^{\alpha}, \tag{14}$$

where $\alpha > 1$ is the correlation exponent.

Similar to rectangle systems [18], we roughly classify the binary ellipse systems into three categories: weakly correlated systems (roughly $a_1 < 2a_2$), strongly correlated systems ($a_1 \approx 2a_2$ and usually $r_1 > 10$), and ultrastrongly correlated systems (roughly $a_1 > 2a_2$ and $r_1 > 10$). The threshold of all systems belonging to the first two categories can be precisely predicted by Eq. (14) with the common correlation exponents $\alpha = 1.5$ and $\alpha = 2.5$ for weakly and strongly correlated systems, respectively. As shown in Fig. 6, the difference between calculated N_c and simulated N_c is negligible (maximum deviation < 0.06). However, for ultrastrongly correlated systems (Fig. 7), because the effective average excluded area $\tilde{\ }$ is often beyond the region [$\tilde{\ }$, $\tilde{\ }$], Eq. (13) cannot accurately estimate N_{ci} and hence Eq. (14) cannot precisely predict N_c for such systems.

C. Threshold symmetry in binary systems

According to the conjecture by Consiglio *et al.* [19], for heterogeneous systems comprising unequal circles (spheres), their critical area (volume) fraction ϕ_c is a symmetric function of the areal (volumetric) fraction v. With respect to the notation in this work, ϕ_c and v are defined, respectively, as

$$\phi_c = 1 - e^{\eta_c},\ \eta_c = N_1S_1 + N_2S_2 = N_c\left(x_1S_1 + x_2S_2\right) \tag{15}$$

and

$$v = \frac{N_1 S_1}{N_1 S_1 + N_2 S_2} = \frac{x_1 S_1}{x_1 S_1 + x_2 S_2} = \frac{\lambda x_1}{1 + (\lambda - 1) x_1}, \tag{16}$$

where $S_i = \pi a_i b_i$, N_i, and $x_i = N_i/N$ with $N = N_1 + N_2$ (note at criticality $N = N_c$) are the area, number density and number fraction of ith type of ellipses, respectively and $\lambda = S_1/S_2$. Consiglio *et al.* [19] expected and roughly demonstrated in all heterogeneous systems consisting of unequal circles (or spheres) the percolation threshold symmetry as

$$\phi_c(v, \lambda) = \phi_c(1 - v, \lambda), \tag{17}$$

which suggests for any λ, ϕ_c is symmetric about v, and reaches maximum *exactly* at v = 1/2. They argued that under the transformation $\hat{N}_1 = \lambda N_2$ and $\hat{N}_2 = \lambda^{-1} N_1$, the new areal fraction is $\hat{v} = 1 - v$ but still $\hat{\phi}_c = \phi_c$, so that Eq. (17) is proven.

Quintanilla and Ziff [17] later pointed out the two flaws in the argument above: (1) after the transformation, although the volume fraction $\eta = N_1 S_1 + N_2 S_2$ is not changed, it does not mean the critical threshold η_c still retains since the criticality depends on more factors than certain volume fraction; and (2) after the transformation, the total number N is changed to $\hat{N} = \lambda^{-1} N_1 + \lambda N_2$, but there is no justification that η_c should remain unaltered after such change of N. Nevertheless, while Quintanilla and Ziff disproved the exact percolation threshold symmetry conjectured by Consiglio *et al.*, their simulation results [17] indeed exhibit fairly good symmetry of ϕ_c about $v \approx 1/2$ for all binary systems consisting of unequal circles.

In this work we investigate the percolation threshold symmetry for binary ellipse systems. As shown in Figs. 8(a)-8(c), when the two types of ellipses have the same aspect ratios, i.e., $r_1 = r_2$, such as the systems {(0.5, 0.5); (0.1, 0.1)}, {(0.5, 0.1); (0.15, 0.03)} and {(0.5, 0.05); (0.2, 0.02)}, their critical area fraction ϕ_c exhibits good symmetry about $v \approx 1/2$. However, once $r_1 \neq r_2$, the symmetry disappears, as shown in Figs. 8(d) and 8(e). We thereby propose to modify

the conjecture in [19] by replacing the ellipse areas S_i in Eqs. (15) and (16) with quarter of the excluded area $\frac{1}{4}A_{ii} = S_i k_i$ [Eq. (6)], as

$$\phi_{cm} = 1 - e^{\eta_{cm}},\ \eta_{cm} = \frac{1}{4}\left(N_1 A_{11} + N_2 A_{22}\right) = N_c\left(x_1 S_1 k_1 + x_2 S_2 k_2\right) \tag{18}$$

and

$$v_m = \frac{N_1 A_{11}}{N_1 A_{11} + N_2 A_{22}} = \frac{x_1 S_1 k_1}{x_1 S_1 k_1 + x_2 S_2 k_2} = \frac{\lambda_m x_1}{1 + (\lambda_m - 1)x_1} \tag{19}$$

where $\lambda_m = A_{11} / A_{22} = S_1 k_1 / S_2 k_2$. As shown in Figs. 8(f)-8(j), for all the binary systems, ϕ_{cm} exhibits good symmetry about $v_m \approx 1/2$, no matter whether r_1 equals to r_2 or not. Actually, one can see $\overline{A} = 4\left(x_1 S_1 k_1 + x_2 S_2 k_2\right)$ roughly as the average excluded area of the binary system. Under the transformation $\hat{x}_1 = \lambda_m^{-1} x_2$ and $\hat{x}_2 = \lambda_m x_2$, while v_m is changed to $\hat{v}_m = 1 - v_m$, $\overline{A}$ remains unaltered. Since *the critical number density N_c is predominated by the average excluded area*, one can expect $\hat{N}_c \approx N_c$ even though the total number density $N = N_1 + N_2$ may change after the transformation. Because both $\overline{A}$ and N_c are not changed upon the transition from v_m to $1-v_m$, $\eta_{cm} = N_c \overline{A} / 4$ and hence ϕ_{cm} do not change either, that is to say,

$$\phi_{cm}\left(v_m, \lambda_m\right) = \phi_{cm}\left(1 - v_m, \lambda_m\right). \tag{20}$$

The derivation of Eq. (20) does not suffer from flaws argued by Quintanilla and Ziff [17]. Instead, Eq. (20) may provide theoretical backing for the percolation threshold symmetry observed in binary circle systems and extend it to general ellipse systems. From Eqs. (7) and (8), the factor k_i only depends on the ellipse aspect ratio r. Therefore, if the two types of ellipses have the same aspect ratio, i.e., $r_1 = r_2$, one has $k_1 = k_2$. Then, v_m in Eq. (19) reduces to v in Eq. (16), and η_{cm} and ϕ_{cm} in Eq. (18) respectively reduce to η_c and ϕ_c in Eq. (15), possibly with a trivial constant shift. In this case, the symmetry of ϕ_{cm} in Eq. (20) gives rise to the symmetry of

ϕ_c in Eq. (17). In our opinion, in essence and in general, there is no percolation threshold (or critical area fraction ϕ_c) symmetry about v, as also claimed by Quintanilla and Ziff. Only in the special case ($r_1 = r_2$), the universal symmetry of ϕ_{cm} about v_m reduces to an apparent symmetry of ϕ_c about v. We believe this is the underlying physics for the percolation threshold symmetry observed in unequal circle ($r_1 = r_2 = 1$) systems [17,19]. However, our derivation of Eq. (20) involves some approximations, such as the rough average excluded area $\bar{A}$ and the universal yet "inexact" relation [24,25] between critical number density and excluded area. Therefore, the symmetry in Eq. (20) should not be exact. This has also been justified by Quintanilla and Ziff [17].

IV. CONCLUSIONS

This work employs and generalizes Vieillard-Baron's contact function and integrates it into our high-efficiency Monte Carlo algorithm to explore 2D homogeneous and heterogeneous random systems comprising overlapping ellipses. High-precision percolation thresholds are reported for various homogeneous ellipse systems with different aspect ratios. A high-order polynomial is proposed to precisely predict threshold for homogeneous ellipse systems of *any aspect ratio ranging from 1 to* ∞ with maximum uncertainty $< 5\times10^{-5}$. In addition, with the concept of modified excluded area, a general law [Eq. (14)] is verified for precise prediction of percolation threshold for binary ellipse systems where the semi-major axis of the longer ellipses is no more than twice that of the shorter ellipses. In particular, based on the extensive study of binary ellipse systems, we derive a universal symmetry [Eq. (20)] concerning excluded area and critical number density, which should provide true physics to the apparent percolation threshold symmetry observed earlier in systems comprising unequal circles.

ACKNOWLEDGEMENT

Most simulations were performed on resources provided by the Swedish National Infrastructure for Computing (SNIC) at C3SE (Project SNIC 2014/1-383) and PDC (Project 1401-006). We acknowledge the financial support by the Göran Gustafsson Foundation through the Young Researcher Prize (No. 1415B), the Olle Engkvist Byggmästare Foundation through the Research Project (No. 2014/799), the European Research Council through the Proof of Concept Grant iPUBLIC (No. 641416), the Swedish Research Council through the research project iGRAPHENE and the Framework project (No. 2014–6160), the Swedish Innovation Agency VINNOVA through the Strategic Innovation Program for Graphene, iEnergy (No. 2015-01337). We also acknowledge the Marie Skłodowska Curie International Career Grant co-funded by the Swedish Research Council (through the Project No. 2015-00395) and Marie Skłodowska Curie Actions (through the Project INCA 600398).

[1] W. Xia, M.F. Thorpe, Percolation properties of random ellipses, Phys. Rev. A. 38 (1988) 2650–2656.

[2] Y.-B. Yi, A.M. Sastry, Analytical approximation of the two-dimensional percolation threshold for fields of overlapping ellipses, Phys. Rev. E. 66 (2002) 066130.

[3] J.-R. de Dreuzy, P. Davy, O. Bour, Percolation parameter and percolation-threshold estimates for three-dimensional random ellipses with widely scattered distributions of eccentricity and size, Phys. Rev. E. 62 (2000) 5948–5952.

[4] J. Cuesta, D. Frenkel, Monte Carlo simulation of two-dimensional hard ellipses, Phys. Rev. A. 42 (1990) 2126–2136.

[5] J. Vieillard-Baron, Phase Transitions of the Classical Hard-Ellipse System, J. Chem. Phys. 56 (1972) 4729-4744.

[6] Y.-B. Yi, A.M. Sastry, Analytical approximation of the percolation threshold for

overlapping ellipsoids of revolution, Proc. R. Soc. London A Math. Phys. Eng. Sci. 460 (2004) 2353–2380.

[7] J. Li, M.C. Lemme, M. Östling, Inkjet Printing of 2D Layered Materials., Chemphyschem. 15 (2014) 3427–3434.

[8] X. Wang, L. Zhi, K. Mullen, Transparent, Conductive Graphene Electrodes for Solar Cells, Nano Lett. 8 (2007) 323–327.

[9] J. Li, F. Ye, S. Vaziri, M. Muhammed, M.C. Lemme, M. Östling, Efficient Inkjet Printing of Graphene, Adv. Mater. 25 (2013) 3985–3992.

[10] J. Li, M.M. Naiini, S. Vaziri, M.C. Lemme, M. Östling, Inkjet Printing of MoS 2, Adv. Funct. Mater. 24 (2014) 6524–6531.

[11] E.S. Snow, J.P. Novak, P.M. Campbell, D. Park, Random networks of carbon nanotubes as an electronic material, Appl. Phys. Lett. 82 (2003) 2145–2147.

[12] J. Li, T. Unander, A. López Cabezas, B. Shao, Z. Liu, Y. Feng, et al., Ink-jet printed thin-film transistors with carbon nanotube channels shaped in long strips, J. Appl. Phys. 109 (2011) 084915.

[13] D.J. Finn, M. Lotya, J.N. Coleman, Inkjet Printing of Silver Nanowire Networks, ACS Appl. Mater. Interfaces. 7 (2015) 9254–9261.

[14] J. Li, M. Östling, Conductivity scaling in supercritical percolation of nanoparticles – not a power law, Nanoscale. 7 (2015) 3424–3428.

[15] J. Li, S.-L. Zhang, Finite-size scaling in stick percolation, Phys. Rev. E. 80 (2009) 040104.

[16] S. Mertens, C. Moore, Continuum percolation thresholds in two dimensions, Phys. Rev. E. 86 (2012) 061109.

[17] J. A. Quintanilla, R.M. Ziff, Asymmetry in the percolation thresholds of fully penetrable disks with two different radii, Phys. Rev. E. 76 (2007) 051115.

[18] J. Li, M. Östling, Percolation thresholds of two-dimensional continuum systems of rectangles, Phys. Rev. E. 88 (2013) 012101.

[19] R. Consiglio, R.N. A. Zouain, D.R. Baker, G. Paul, H.E. Stanley, Symmetry of the continuum percolation threshold in systems of two different size objects, Physica A. 343 (2004) 343–347.

[20] M. Newman, R. Ziff, Efficient Monte Carlo Algorithm and High-Precision Results for Percolation, Phys. Rev. Lett. 85 (2000) 4104–4107.

[21] T. Vicsek, J. Kertesz, Monte Carlo renormalisation-group approach to percolation on a continuum: test of universality, J. Phys. A. Math. Gen. 14 (1999) L31–L37.

[22] R.M. Ziff, Spanning Probability in 2D Percolation, Phys. Rev. Lett. 69 (1992) 2670–2673.

[23] J.P. Hovi, A. Aharony, Renormalization group, scaling and universality in spanning probability for percolation, Phys. Rev. E. 53 (1995) 235–253.

[24] I. Balberg, C.H. Anderson, S. Alexander, N. Wagner, Excluded volume and its relation to the onset of percolation, Phys. Rev. B. 30 (1984) 3933–3943.

[25] I. Balberg, Universal percolation-threshold limits in the continuum, Phys. Rev. B. 31 (1985) 4053–4055.

[26] C. Mack, The expected number of clumps when convex laminae are placed at random and with random orientation on a plane area, Math. Proc. Cambridge Philos. Soc. 50 (1954) 581-585.

[27] C. Mack, On clumps formed when convex laminae or bodies are placed at random in

two or three dimensions, Math. Proc. Cambridge Philos. Soc. 52 (1956) 246-250.

[28] T.R. Chandrupatla, T.J. Osler, The perimeter of an ellipse, Math. Sci. 35 (2010) 122–131.

[29] J. Li, Erratum: Percolation thresholds of two-dimensional continuum systems of rectangles [Phys. Rev. E 88, 012101 (2013)], arXiv:1604.01315v1 (2016).

[30] A.P. Chatterjee, Percolation Thresholds and Excluded Area for Penetrable Rectangles in Two Dimensions, J. Stat. Phys. 158 (2015) 248–254.

TABLE I. Percolation thresholds N_c obtained from Monte Carlo simulations for FBC and PBC homogeneous systems comprising overlapping ellipses with various aspect ratios r, the excluded area A_r for the ellipses, and their product N_cA_r. Since N_c (FBC) is very close to N_c (PBC), they do not give evident distinction in the calculated N_cA_r.

r	N_c (FBC)	N_c (PBC)	Nc from the literature	A_r	$N_c A_r$
1	1.436 340 (17)	1.436 323 (3)	1.436 325 48 (7) [16]	π	4.5123
1.5	2.059 093 (19)	2.059 081 (7)		2.1600	4.4476
2	2.523 583 (35)	2.523 560 (8)	2.5 [1]	1.7191	4.3383
3	3.157 353 (39)	3.157 339 (8)	3.1 [1]	1.3133	4.1465
4	3.569 713 (37)	3.569 706 (8)	3.5 [1]	1.1247	4.0149
5	3.861 252 (27)	3.861 262 (12)	3.86 [6]	1.0167	3.9258
6	4.079 359 (20)	4.079 373 (17)		0.9471	3.8634
7	4.249 158 (39)	4.249 132 (16)		0.8986	3.8182
8	4.385 303 (22)	4.385 302 (15)		0.8630	3.7843
9	4.497 044 (25)	4.497 000 (8)		0.8357	3.7582
10	4.590 428 (19)	4.590 416 (23)	4.56 [6]	0.8142	3.7376
15	4.894 745 (30)	4.894 759 (30)		0.7516	3.6787
20	5.062 310 (54)	5.062 313 (39)	4.99 [6]	0.7214	3.6517
30	5.241 522 (31)	5.241 510 (26)		0.6920	3.6272
50	5.393 860 (56)	5.393 863 (28)	5.38 [6]	0.6693	3.6099
100	5.513 493 (67)	5.513 464 (40)	5.42 [6]	0.6527	3.5985
500	5.612 260 (63)	5.612 259 (30)		0.6398	3.5906
1000	5.624 732 (88)	5.624 756 (22)	5.5 [6]	0.6382	3.5897
∞			5.637 263 (11) (FBC) [15] 5.637 285 8(6) (PBC) [16]	$2\pi^{-1}$	3.5888

TABLE II. Coefficients for the nonlinear regression of Eqs. (9) and (12) to the simulated N_c (PBC) in Table I. The uncertainty is the half-width of the 95% confidence interval from the nonlinear regression. All coefficients are rounded to five decimal places, which are needed for the calculation of precise N_c through Eq. (9) or (12), although their uncertainty does not really support such a precision of five decimal places.

i	c_i [Eq. (9)]	Uncertainty (c_i)	$\tilde{c}_i$ [Eq. (12)]	Uncertainty ($\tilde{c}_i$)
1	5.94966	0.02	5.49735	0.06
2	14.63149	0.2	10.38148	0.8
3	–66.24868	1.2	–44.1784	4.7
4	136.84951	3.7	90.71676	13.9
5	–169.18819	6.4	–117.81399	23.7
6	128.84490	6.5	99.08025	23.4
7	–55.69872	3.5	–48.69805	12.4
8	10.49732	0.8	10.65185	2.7

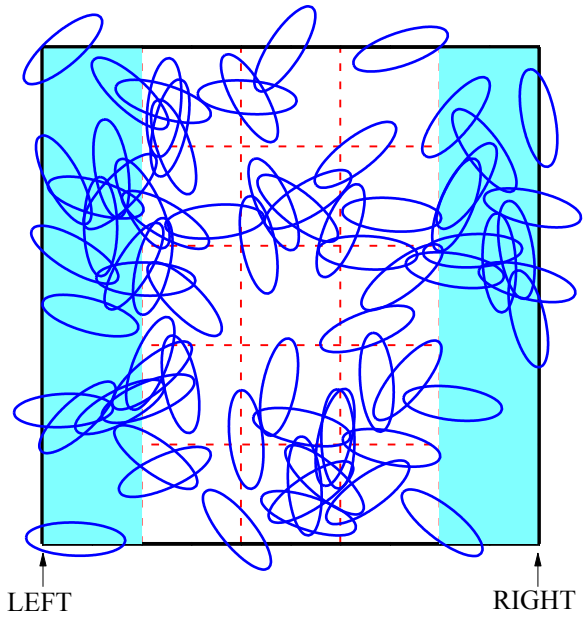

FIG. 1. Snapshot of a percolated homogeneous FBC percolation system consisting of randomly-distributed overlapping ellipses, as produced by our Monte Carlo simulation program. All the ellipses are of semi-major axis $a = 0.5$ and aspect ratio $r = 3$. The system (of size $L = 5$ in this figure) percolates when its two boundaries, labelled respectively as "LEFT" and "RIGHT" and treated as "fake" ellipses in our algorithm, are connected by intersecting ellipses (like the case in this figure).

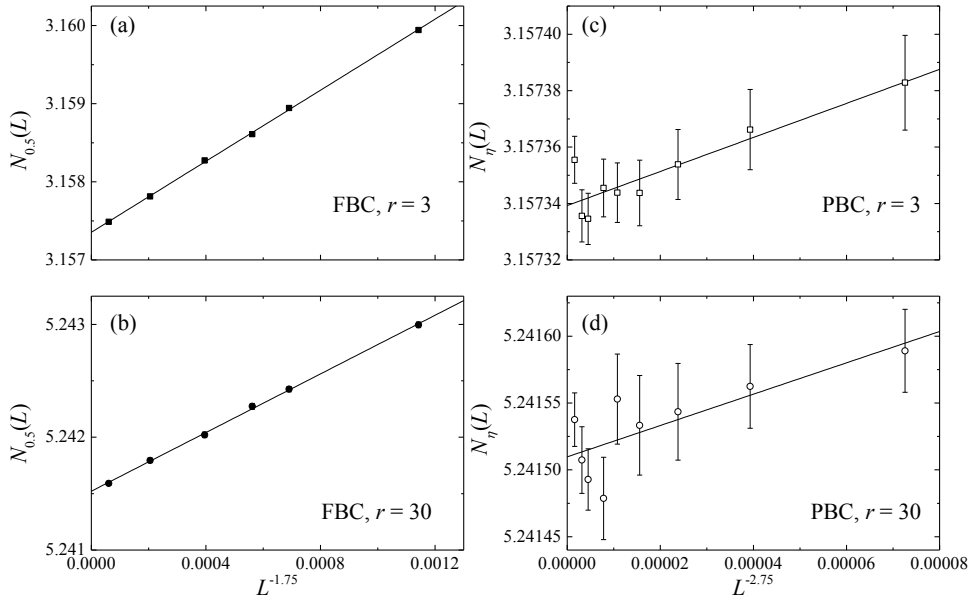

FIG. 2. Plots of $N_{0.5}(L)$ against $L^{-1-1/\nu}$ for FBC ellipse systems of (a) $r = 3$ and (b) $r = 30$, and $N_\eta(L)$ against $L^{-2-1/\nu}$ for PBC ellipse systems of (c) $r = 3$ and (d) $r = 30$. The error bars are given by $\sigma_{N_\eta} = \sigma_P \big/ P'\left[N_\eta(L)\right] = \sqrt{P_\infty(1-P_\infty)}m^{-1/2} \big/ P'\left[N_\eta(L)\right]$ where P stands for the spanning probability R for FBC systems and the wrapping probability W for PBC systems, m is the number of simulation runs [16], and for FBC systems in (a) and (b), N_η stands for $N_{0.5}$ and the error bars are smaller than the symbols.

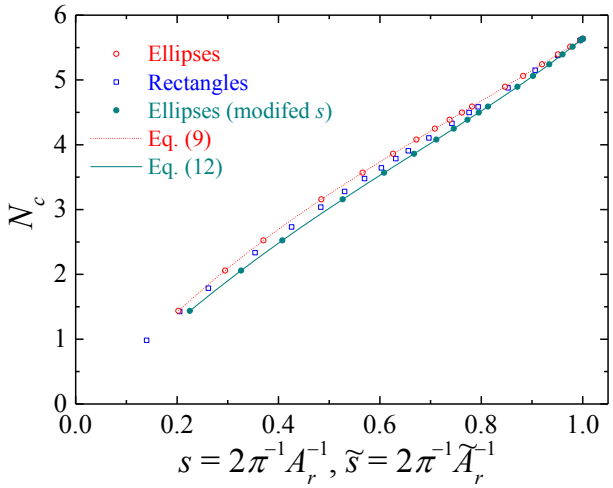

FIG. 3. Plots of simulated N_c (symbols) against s or $\tilde{s}$ for homogeneous ellipse systems and rectangle systems [18]. The systems are measured by the major axis of ellipses or the length of rectangles. All the error bars (uncertainty) are far smaller than the symbols. The curves are nonlinear regression by Eqs. (9) and (12), respectively.

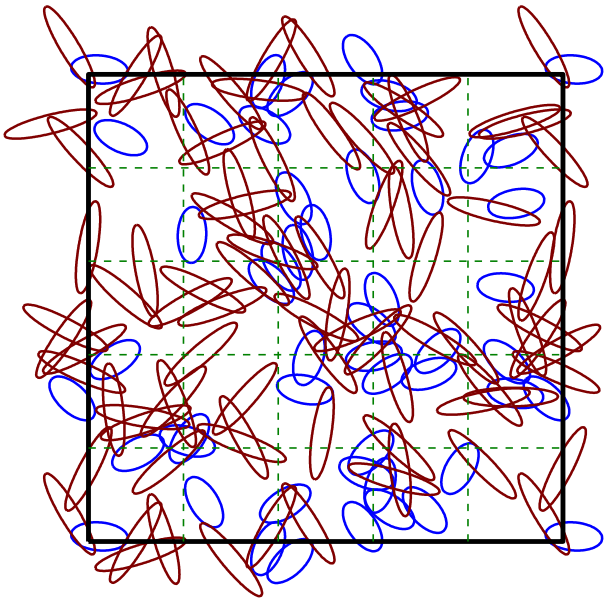

FIG. 4. Snapshot of a wrapped binary PBC ellipse system [(0.5, 0.1), 0.6; (0.3, 0.15), 0.4]. The system size is L = 5. Note that both the horizontal and vertical boundaries are periodic. The system in this figure is wrapped by intersecting ellipses both horizontally and vertically.

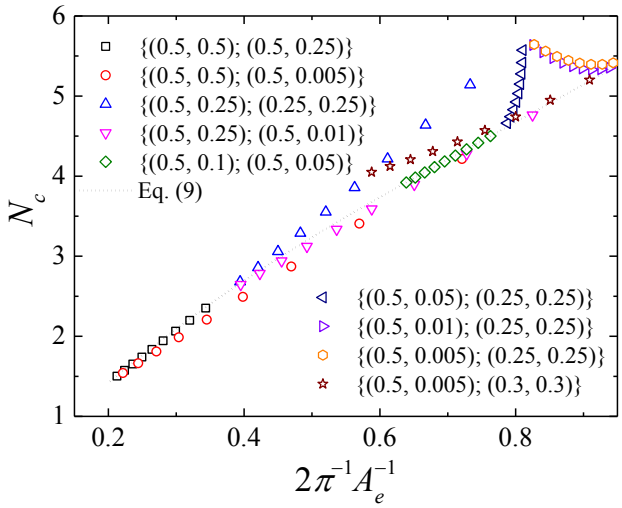

FIG. 5. Plots of simulated N_c (symbols) against $s = 2\pi^{-1}A_e^{-1}$ for a variety of heterogeneous (binary) ellipse systems. All N_c is approximated by $N_\eta(L = 32)$. The dotted curve is given by Eq. (9).

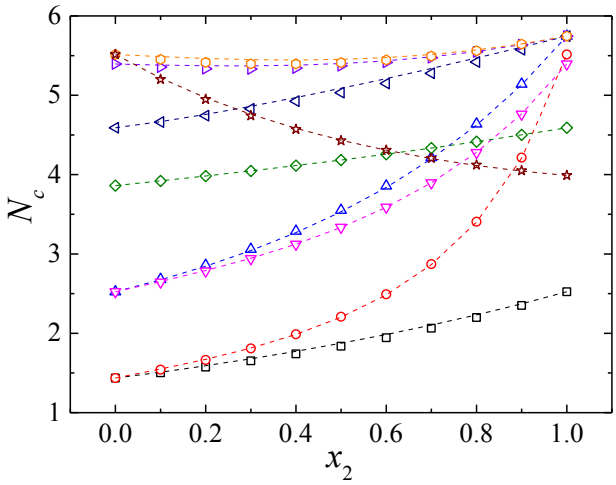

FIG. 6. Percolation thresholds obtained from simulations (symbols) and calculations through Eq. (14) (dashed curves) for different binary systems. The symbols have the same legends as in Fig. 5. For the calculations through Eq. (14), $\alpha = 2.5$ for the systems {(0.5, 0.01); (0.25, 0.25)} and {(0.5, 0.005); (0.25, 0.25)}, and $\alpha = 1.5$ for all the other systems. For the systems {(0.5, 0.05); (0.25, 0.25)}, $\alpha = 2.5$ and $\alpha = 1.5$ give almost identical results. All N_c is approximated by $N_\eta(L = 32)$.

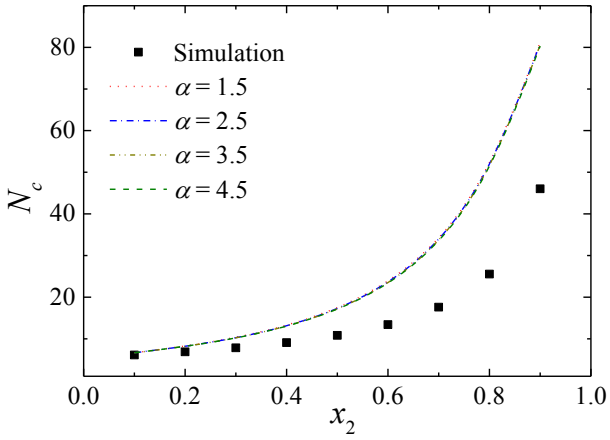

FIG. 7. Percolation thresholds obtained from simulations (squares) and calculations through Eq. (14) (dashed curves) for the systems {(0.5, 0.005); (0.05, 0.05)}. In these ultrastrongly correlated systems, Eq. (14) with any α cannot give satisfactory fitting to the simulations. All N_c is approximated by $N_\eta(L=32)$.

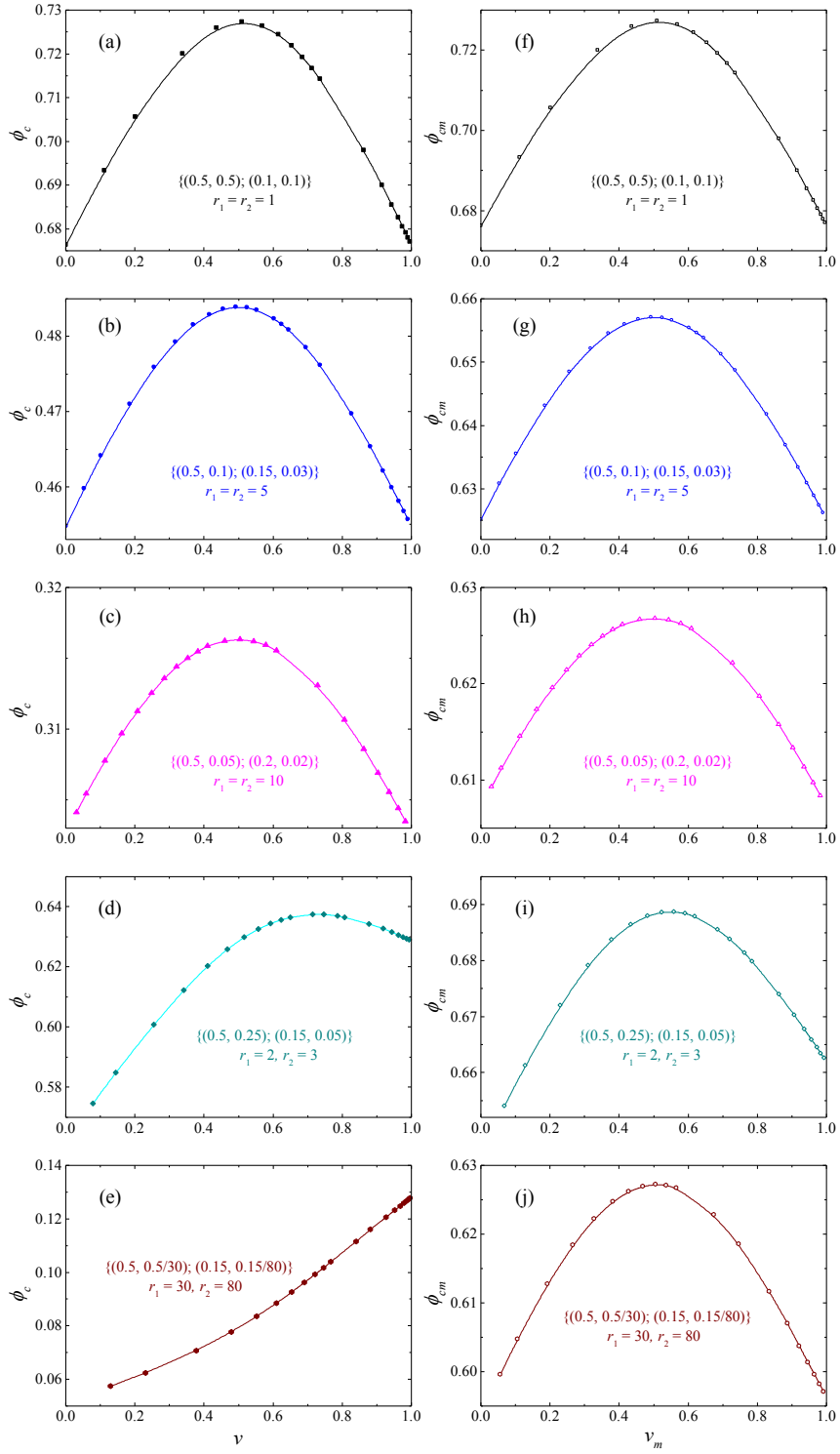

FIG. 8. Plots of (a-e) ϕ_c against v and (f-j) ϕ_{cm} against v_m for five different groups of binary ellipses systems. In the calculation of ϕ_c and ϕ_{cm}, all the critical number density N_c is approximated by $N_\eta(L = 32)$.